

## Original Article

# Generation of homologous cell pairs using the oral lymphatic system

Yin-Fei Pu<sup>1</sup>, Lin Wang<sup>1</sup>, Huan-Huan Wu<sup>1</sup>, Huan Bian<sup>1</sup>, Ying-Ying Hong<sup>2</sup>, Yi-Xiang Wang<sup>3</sup>, Chuan-Bin Guo<sup>1</sup>

<sup>1</sup>Department of Oral and Maxillofacial Surgery, Peking University School and Hospital of Stomatology, Beijing, China; <sup>2</sup>Department of Pathology, Peking University School and Hospital of Stomatology, Beijing, China; <sup>3</sup>Central Laboratory, Peking University School and Hospital of Stomatology, Beijing, China

Received January 23, 2014; Accepted March 10, 2014; Epub March 15, 2014; Published April 1, 2014

**Abstract:** The purpose of this study is to establish in vivo and in vitro models for studying lymphatic metastasis of squamous cell carcinoma (SCC). Three cell lines CAL-27, Tca-83, and HeLa were injected into the tongue of nude mice. Forty days after injection, we could isolate cells of 2 homologous cell lines LN-CAL-27 and LN-HeLa from lymph node metastasis lesions. Then, the homologous cell pairs were compared by the CCK-8 assay, wound healing assay, real-time PCR, western blot, and animal experiments. The results showed that all the three cell lines could be used to establish lymphatic metastasis animal models, and the lymphatic metastasis process was observed clearly. In addition, the homologous cell pairs performed differently from parent lines with respect to biological behavior and lymphatic metastasis-related gene and protein expression. In conclusion, CAL-27, Tca-83, and HeLa cells could be used to simulate the lymphatic metastasis process of oral cancer in vivo. Furthermore, the homologous cell pairs (CAL-27 and LN-CAL-27; HeLa and LN-HeLa) are potential tools for in vitro investigation of the mechanisms underlying metastasis.

**Keywords:** Oral cancer, lymphatic metastasis, animal model, oral lymphatic system, homologous cell pair

## Introduction

Lymphatic metastasis is the most common metastatic route for some types of cancer, especially for SCC, which is most likely to invade the lymphatic system, spread to regional lymph nodes, and ultimately spread to other parts of the body [1, 2]. SCC accounts for more than 90% of oral cancers [3], and its metastasis to lymph nodes is the major cause of mortality for this disease [4]. Despite advances in treatment, the 5-year survival rate of oral cancer still remains at 60% and has not improved significantly over the past several decades [5]. Furthermore, the 5-year survival rate is less than 28% in patients diagnosed with oral SCC with lymphatic metastasis [6].

In the past 10 years, along with identification of lymphatic specific markers [7], more attention has been paid to investigating the mechanism underlying lymphatic metastasis of SCC [8]. However, the mechanism still remains largely unknown because scientists lack a reliable

model that can simulate the complicated process. In previous studies, researchers have used oral or footpad lymphatic systems to study lymphatic metastasis. Qiu et al. transplanted human tumor specimens into the tongues of nude mice, dissected the metastatic lymph nodes, and again transplanted the tissue into the tongues; the metastatic rate increased significantly in the fourth round [9]. Myers et al. injected Tu167 cells transfected with the green fluorescent protein gene into the tongues of nude mice; metastatic tumor cells from lymph nodes were harvested and again injected into the tongues of nude mice to identify the ability for metastasis [10]. Sano et al. used luciferase-transduced cells to inoculate the tongues of the nude mice [11] for improving detection of lymphatic metastasis.

In this study, we used 3 cell lines to establish a lymphatic metastasis animal model of oral cancer and for pathological analysis of the lymphatic metastasis process. In addition, we cultured 2 homologous cell pairs with differing biological

## In vivo and in vitro lymphatic metastasis models

behaviors, gene and protein expression, and metastatic rates.

### Materials and methods

#### *Cells and cell culture*

The human oral tongue squamous cell line CAL-27 and cervical carcinoma cell line HeLa and their derivative homologous cell lines LN-CAL-27 and LN-HeLa were maintained in Dulbecco's Modified Eagle's Medium (DMEM; Gibco), and the human oral tongue squamous cell line Tca-83 was maintained in RPMI-1640 (Gibco), supplemented with 10% fetal bovine serum (FBS; Hyclone), in a humidified 5% CO<sub>2</sub> incubator at 37°C. Cells in mid-logarithmic growth (~75% confluence) were used for the following experiments. All the three cell lines were cultured carefully to prevent cross contamination.

#### *Establishment of the SCC lymphatic metastasis animal model in nude mice*

This study was approved by the Medical Ethical Committee of the Peking University School and Hospital of Stomatology (LA 2012-79). Six-week-old male nude mice (Vital River Laboratory Animal Technology Co. Ltd., Beijing, China) were placed under general anesthesia with 1% pentobarbital sodium (Sigma). SCC cells ( $5 \times 10^6$ ) were injected into the right side of the anterior third of the tongue (tongue group) and footpad (footpad group). Fifteen days after injection, a nutritious semi-liquid diet was provided to the tongue group to alleviate weight loss due to tumor growth in the tongue. After 40 days for the tongue group and 60 days for the footpad group, mice were sacrificed with an overdose of pentobarbital sodium, and the cervical and popliteal swollen lymph nodes were dissected and divided in half. One half was used in tissue culture to generate lymph node-derived homologous cell lines, and the other was fixed immediately with 4% paraformaldehyde for pathological analysis.

#### *Detection of lymphatic metastatic foci*

Swollen lymph nodes and primary tumors were embedded in wax for pathological analysis. Then, 4- $\mu$ m-thick sections were mounted on slides for hematoxylin and eosin (HE) staining and immunohistochemical staining. After dewaxing, the slides were stained with HE or treated with 3% hydrogen peroxide for 10 min

to block the endogenous peroxidase activity. Antigen retrieval was performed using a high pressure method (citrate, 0.01M, pH 6.0) for 3 min. The slides were incubated with the epithelial marker pan-cytokeratin (pan-CK; ready-to-use; Zhongshanggoldenbrige Co. Ltd, Beijing, China, ZM-0067) in a humidified chamber overnight at 4°C, and they were incubated with horseradish peroxidase (HRP)-conjugated secondary antibody for 1 h at ambient temperature. After washing, the immunoreaction was followed by incubation with diaminobenzidine (DAB, Zhongshanggoldenbrige Co. Ltd.) for 30 s. The slides were counterstained with hematoxylin, and images were recorded by an Olympus DP controller (Olympus, Japan).

#### *Generation of lymph node-derived homologous cell lines*

The swollen lymph nodes were cut into small fragments (less than 1 mm<sup>3</sup>) for tissue culture and cultured in a T25 flask with DMEM containing 10% FBS, at 37°C in a humidified 5% CO<sub>2</sub> atmosphere. Single colony-derived cell lines were established and cultured continuously over 60 passages, and then identified by Goldeneye™ 20A Short Tandem Repeat (STR) profiling.

#### *Cell proliferation assay*

Cell proliferation was measured in vitro with the CCK-8 assay (Dojindo). Briefly,  $3 \times 10^3$  cells were plated into 96-well plates with 100  $\mu$ L growth medium per well. Following overnight incubation, cells were cultured in DMEM containing 10% FBS or serum-free DMEM. Every 24 hours, 10  $\mu$ L CCK-8 solution was added to each well, and the cultures were incubated for 2 h at 37°C. Color development was quantified photometrically at 450 nm using an ELx808 absorbance microplate reader (Bio TeK Instruments). All the experiments were performed in biological triplicates and were repeated at least 3 times.

#### *Wound healing assay*

Cells ( $5 \times 10^5$ ) were cultured as confluent monolayers and were wounded by scratching across the well with a 200  $\mu$ L pipette tip. The deciduous cells were removed by D-Hanks. At 0, 24, and 48 h after wounding, the monolayers were photographed at 10  $\times$  magnification (Nikon, Japan) and the distance between the

## In vivo and in vitro lymphatic metastasis models

**Table 1.** The sequences of real-time PCR primers used in this study

Gene	Forward primers	Reverse primers
CCL14	GGGACCTTACCACCCCTCA	GCTGACGCGGGATCTTGTA
CCL15	TCCCAGGCCAGTTCATAAAT	TGCTTTGTGAGATGTAGGAGGT
CCL19	CCAGCCCCAACTCTGAGTG	ATCCTTGATGAGAAGGTAGTGGA
CCL2	GATCTCAGTGCAGAGGCTCG	TGCTTGCCAGGTGGTCCAT
CCL21	AGCCTCCTTATCCTGGTTCTG	ACAACCTTGGCGGGAATCTTC
CCL23	ACTTCTGGACAGATCCATGCT	CTTCGTGGGGTGTAGGAGATG
CCL27	TCCTGAGCCCAGACCCTAC	CAGTTCACCTGGATGACCTT
CCL28	TGCACGGAGGTTTCACATCAT	ACAGATTCTTCTGCGCTTGAC
CXCL10	GTGGCATTCAAGGAGTACCTC	GCCTTCGATTCTGGATTACAGACA
CXCL11	TTGGCTGTGATATTGTGTGCT	GGATTAGGCATCGTTGTCCTTT
CXCL12	ATGCCATGCCGATTCTTCG	GCCGGGCTACAATCTGAAGG
CXCL13	TTGAGGTGTAGATGTGTCCAAGA	ATTGCATCAATGAAGCGTCTAGG
CXCL14	GGACCCAAGATCCGCTACAG	TCCAGGGTGTGACCACTTG
CXCL16	CAGCGTACTGGAAGTTGTTA	CACCGATGGTAAGCTCTCAGG
CXCL5	GAGAGCTGCGTTGCGTTTG	TTTCTTGTTCACCGTCCA
CXCL6	AGAGCTGCGTTGCACTTGTT	GCAGTTTACCAATCGTTTTGGGG
CXCL9	CCAGTAGTGAGAAAGGGTCGC	TGGGGCAAATTGTTAAGGTCTT
CXCR1	GCAGCTCCTACTGTTGGACA	GGGCATAGGCGATGATCACA
CXCR2	AGCTGAGAATATGCAGCCGTT	GAGACCACCTTGACAGGAA
CXCR4	ATGAAGGAACCCTGTTCCGT	AGATGATGGAGTAGATGGTGGG
HIF1 $\alpha$	ACTTGCAACCTTGATTGGA	GCACCAAGCAGGTCATAGGT
IL24	TTGCTGGGTTTTACCCTGC	AAGGCTTCCACAGTTTCTGG
MMP-13	TTTCAACGGACCCATACAGTTTG	CATGACGCGAACAATACGTTA
MMP-14	GAAGCCTGGCTACAGCAATATG	TGCAAGCCGTAACCTTCTGC
MMP-16	GCTGTGATGGACCAACAGACA	CCAAGATGCAGGGAATGACAA
MMP-25	GACTGGCTGACTCGCTATGG	CGAACCTCTGCATGACTTTGATG
MMP-2	GCCCCAGACAGGTGATCTTG	GCTTGCAGGGAAGAAGTTGT
MMP-7	CATGAGTGAGCTACAGTGGGA	CTATGACGCGGGAGTTAACAT
MMP-9	GCCCGACCCGAGCTGACTC	TTCAGGGCGAGGACCATAGAGG
periostin	GAAGGAATGAAAGGCTGCCCA	GAATCCAAGTTGTCCAAGCC
S100A2	GCCAAGAGGGGCGACAAGTT	AGGAAAACAGCATACTCTGGA
S100A4	GATGAGCAACTTGACAGCAA	CTGGGCTGCTTATCTGGGAAG
S100A5	CACTATGGTGACCACGTTTCA	TCCCCAAGACACAGCTCTTTC
S100A9	GGTCATAGAACACATCATGGAGG	GGCCTGGCTTATGGTGGTG
S100P	ATGACGGAAGTAGAGACAGCC	AGGAAGCCTGGTAGCTCCTT
TNF $\alpha$	GTGCTTGTCTCAGCCTCT	GCTTGTCACTCGGGGTTCTGA
VEGF-A	GCAGAATCATACGAAGTGG	GCAACGCGAGTCTGTGTTTTTG
VEGF-C	ACGTTCCCTGCCAGCAACAC	TCATCCAGCTCCTGTTTGGTCC
VEGF-D	GTGCAGGGCTCCAGTAATGAAC	CCGATGGGATGCTGAGCGAG

front of the removed cells on the wound was measured.

### Real-time PCR

Total RNA was extracted from tumor cells using TRIzol reagent (Invitrogen). Complementary DNA was synthesized by reverse transcription with the GoScript™ Reverse Transcription System (Promega). Relative quantitative PCR

was done using the SYBR Green master mix (Roche Diagnostics). All PCR reactions were performed in a 20  $\mu$ L total volume containing 10  $\mu$ L of SYBR Green PCR master mix, 50 ng cDNA, and 250 nM of each primer (**Table 1**). Relative expression of the target genes was calculated using the  $2^{-\Delta\Delta Ct}$  method.

### Western blot

Cells were lysed in RIPA buffer (Applygen Technologies, Beijing, China) with protease inhibitors (Applygen Technologies). 40  $\mu$ g of protein was loaded onto a polyacrylamide gel for each sample. Proteins were separated by sodium dodecyl sulfate-polyacrylamide gel electrophoresis (Applygen Technologies) and transferred to a polyvinylidene difluoride membrane. The membranes were blocked in 5% non-fat dry milk for 1 h and probed with antibodies against VEGF-C (1:1000 dilution, Abcam), VEGF-D (1:800, Abcam), VEGFR-3 (1:50, Abcam), MMP-2 (1:1000, Epitomics), MMP-9 (1:500, Epitomics), MMP-12 (1:1000, Epitomics), MMP-13 (1:1000, Epitomics), MMP-14 (1:1000, Epitomics), MMP-17 (1:1000, Epitomics), Bcl-2 (1:1000, Genetex), Bad (1:1000, Genetex), BID (1:1000, Genetex), and GAPDH (1:1000, Santa Cruz Biotechnology) separately at 4°C overnight. After incubation

with HRP-linked secondary antibodies, immunoreactive proteins were visualized with an enhanced chemiluminescence reagent (Applygen Technologies).

### Statistical analysis

All results were evaluated with the SPSS 13.0 software. Data are expressed as mean  $\pm$  SD and have been compared using the Student *t*

## In vivo and in vitro lymphatic metastasis models

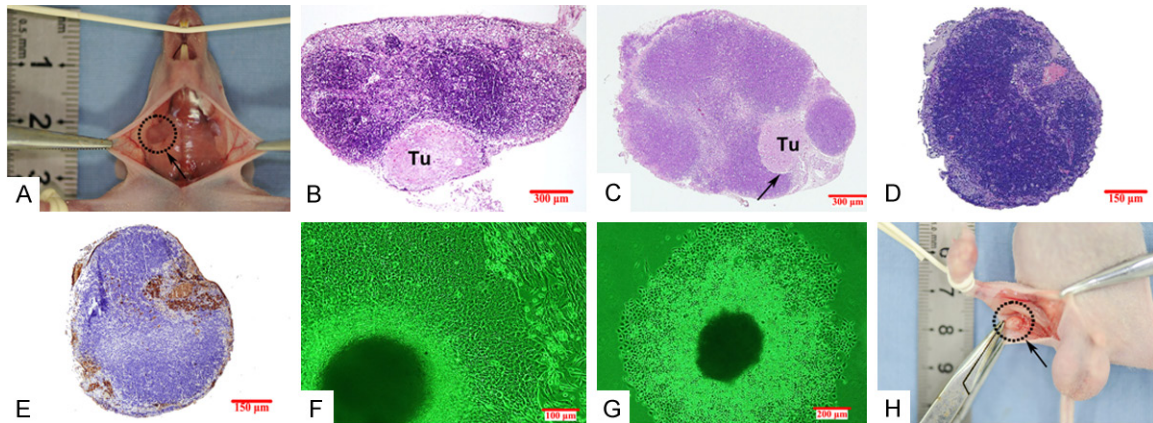


**Figure 1.** Establishment of a lymphatic metastasis animal model and homologous cell pairs via the oral lymphatic system of nude mice. (A) A small white lump embedded in the swollen lymph node denotes lymphatic metastatic foci. (B) Metastatic CAL-27 cells, (C) HeLa cells, and (D) Tca-83 cells are visible in an HE-stained slide. (E) Immunostaining of pan-CK indicates the location of the metastatic Tca-83 cells. (F) LN-CAL-27 cells and (G) LN-HeLa cells were isolated from the neck lymph node metastatic tissue. (H) A swollen popliteal lymph node (black arrow) was found in the popliteal space at day 60 post inoculation. Tu, metastatic tumor cell.

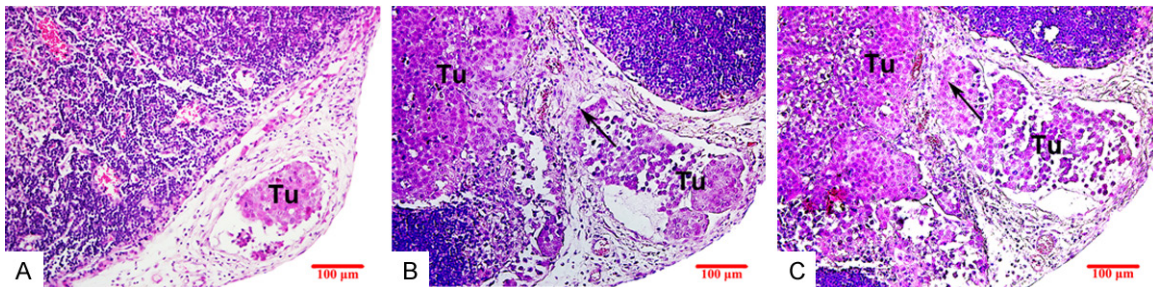


**Figure 2.** Serial sections illustrate the invasive process of tumor cells from the lymphatic vessel into the lymph node. A: Tumor cells in the lymphatic vessel. B: Tumor cells within the expanded lymphatic vessel invade the lymph node. C: Tumor cells invade the partial wall of the lymphatic vessel. Tu, metastatic tumor cell.

tests or ANOVA, as appropriate.  $P < 0.05$  was considered statistically significant.

### Results

#### STR profiling analysis

The 20 gene foci in CAL-27 and LN-CAL-27 are mentioned as follows: [D19S433 (14, 15.2); D5S818 (11, 12); D21S11 (28, 29); D18S51 (13, 13); D6S1043 (12, 12); D3S1358 (16, 16); D13S317 (10, 11); D7S820 (10, 10); D16S539 (11, 12); CSF1PO (10, 12); PentaD (9, 10); Amelogenin (X, X); vWA (14, 17); D8S1179 (13, 15); TPOX (8, 8); PentaE (7, 7); TH01 (6, 9.3); D12S391 (18.3, 19.3); D2S1338 (23, 24); FGA (25, 25)]. All of the 20 gene foci were the same; therefore we concluded that both the cell lines originated from 1 patient. 9 of the gene foci were compared with the foci that provided by

the American type culture collection (ATCC; CRL-2095) and results showed that the cells were not contaminated by others. The other cell lines Tca-83, HeLa, and LN-HeLa cells were also identified by STR analysis (data not shown). Results showed that Tca-83 was not contaminated by other cells. All of the 20 gene foci of HeLa and LN-HeLa cells were the same with each other and 9 of them were the same with the foci that ATCC provided.

#### Evidence for the valuable role of the oral lymphatic system in studying SCC lymphatic metastasis

To observe the process of lymphatic metastasis, CAL-27, Tca-83, and HeLa cells ( $5 \times 10^5$ ) were inoculated into the right side of mice tongue tips. A swollen neck lymph node was clearly observed at 40 d after tumor cell inocu-

## In vivo and in vitro lymphatic metastasis models

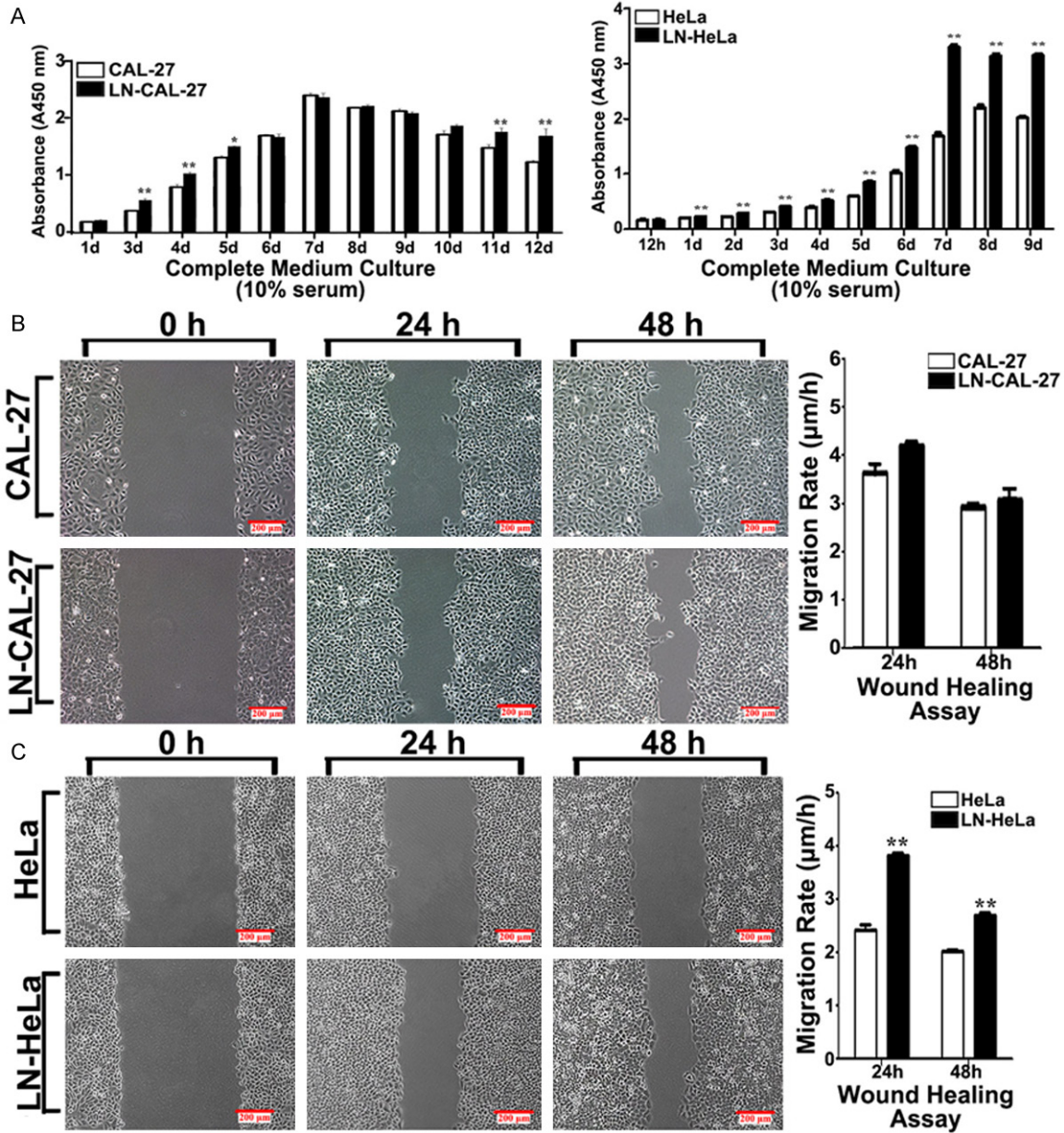


**Figure 3.** Comparison of biological behavior of homologous cell pairs. A: The OD value of the homologous cell pairs. B: Wound healing assay of CAL-27 and LN-CAL-27. C: Wound healing assay of HeLa and LN-HeLa. \*,  $P < 0.05$ ; \*\*,  $P < 0.01$ .

lation, and a small lump of white tumor tissue was enveloped in the lymph node (Figure 1A), which was removed and divided into half for cell culture and pathological analysis. Histopathological analysis by HE staining (Figure 1B-D) showed that all the 3 cell lines metastasized by spreading to the neck lymph node. To identify the metastatic Tca-83 cells, pan-CK tests were performed via immunostaining, and tumor cells strongly expressed pan-CK (Figure 1E). Two novel lymph node-derived homologous cell lines LN-CAL-27 and LN-HeLa

were successfully generated from the LN primary culture of the enlarged neck lymph node (Figure 1F and 1G). In addition, HeLa cells ( $5 \times 10^5$ ) were injected into the footpads of 10 nude mice. However, no metastatic lymph node was detectable in the footpad group, even 60 d after inoculation (Figure 1H).

### Pathological observation of the lymphatic metastasis process

Serial section analysis showed that tumor cells could migrate into the neck lymph nodes by

## In vivo and in vitro lymphatic metastasis models

**Table 2.** Differential expression of 30 genes between LN-CAL-27 and CAL-27 cells and 29 genes between LN-HeLa and HeLa cells

LN-HeLa versus HeLa				LN-CAL-27 versus CAL-27			
Abbreviation	GenBank accession no.	Fold change	P-value	Abbreviation	GenBank accession no.	Fold change	P-value
Increased				Increased			
CCL15	NM_032965.4	4.0	0.036	CCL15	NM_032965.4	2.6	0.049
CXCR2	NM_001168298.1	2.5	0.025	CXCR2	NM_001168298.1	2.5	0.006
CXCR4	NM_003467.2	1.5	0.041	CXCR4	NM_003467.2	1.7	0.019
HIF1 $\alpha$	NM_001243084.1	1.4	0.005	HIF1 $\alpha$	NM_001243084.1	11.2	0.012
MMP-2	NM_001127891.1	1.7	0.049	MMP-2	NM_001127891.1	1.8	0.041
MMP-7	NM_002423.3	2.1	0.008	MMP-7	NM_002423.3	3.0	0.025
MMP-13	NM_002427.3	1.6	0.025	MMP-13	NM_002427.3	3.5	0.004
MMP-14	NM_004995.3	1.4	0.043	MMP-14	NM_004995.3	4.5	0.018
VEGF-C	NM_005429.3	1.6	0.032	VEGF-C	NM_005429.3	1.4	0.039
MMP-9	NM_004994.2	1.5	0.046	VEGF-A	NM_001204385.1	4.0	0.003
CCL2	NM_002982.3	1.6	0.057	CXCL5	NM_002994.4	2.9	0.037
CXCL14	NM_004887.4	2.4	0.044	CXCR1	NM_000634.2	1.7	0.004
IL24	NM_001185158.1	2.2	0.043	S100A2	NM_005978.3	1.8	0.025
Periostin	NM_006475.2	4.6	0.001	S100A4	NM_019554.2	1.3	0.031
				S100P	NM_005980.2	1.5	0.011
Decreased				Decreased			
CCL14	NM_032962.4	6.2	0.001	CCL14	NM_032962.4	4.2	0.065
CXCL6	NM_002993.3	7.7	0.021	CXCL6	NM_002993.3	4.4	0.023
CXCL9	NM_002416.1	16.3	0.009	CXCL9	NM_002416.1	3.3	0.016
CXCL12	NM_000609.6	4.5	0.043	CXCL12	NM_000609.6	4.6	0.023
CXCL13	NM_006419.2	13.3	0.025	CXCL13	NM_006419.2	1.5	0.049
CXCL16	NM_001100812.1	2.5	0.013	CXCL16	NM_001100812.1	1.4	0.027
MMP-25	NM_022468.4	1.7	0.017	MMP-25	NM_022468.4	5.8	0.045
S100A5	NM_002962.1	7.7	0.045	S100A5	NM_002962.1	2.5	0.019
CCL27	NM_006664.2	2.6	0.029	CCL19	NM_006274.2	5.7	0.004
CCL28	NM_148672.2	2.6	0.029	CCL21	NM_002989.3	7.6	0.029
CXCL1	NM_001511.3	10.7	0.055	CCL23	NM_145898.2	1.6	0.046
CXCL5	NM_002994.4	9.1	0.028	CXCL14	NM_004887.4	1.6	0.015
CXCL10	NM_001565.3	2.3	0.019	MMP-16	NM_005941.4	1.9	0.016
CXCL11	NM_005409.4	2.5	0.001	TNF $\alpha$	NM_000594.3	2.3	0.021
S100A9	NM_002965.3	14.1	0.007	VEGF-D	NM_004469.4	4.3	0.025

penetrating the lymphatic vessels. Initially, the wall of the lymphatic vessel containing tumor cells was integrated (**Figure 2A**). Gradually, the lymphatic vessel expanded significantly, and tumor cells invaded and migrated out of the lymphatic vessel. The wall of the lymphatic vessel adjacent to the lymph node center became poorly defined (**Figure 2B**). Ultimately, tumor cells penetrated the lymphatic vessel completely, and there was almost no clear boundary between the tumor cells in the lymphatic vessel and in the lymph node (**Figure 2C**).

*Lymph node-derived cells have higher proliferation, migration abilities than their parental cells*

A CCK-8 assay was performed with complete medium culture (10% serum). The results showed that LN-CAL-27 and LN-HeLa cells had greater proliferative ability than their parental cells (**Figure 3A**).

Spontaneous cell migration was evaluated using the wound healing assay. The migration

## In vivo and in vitro lymphatic metastasis models

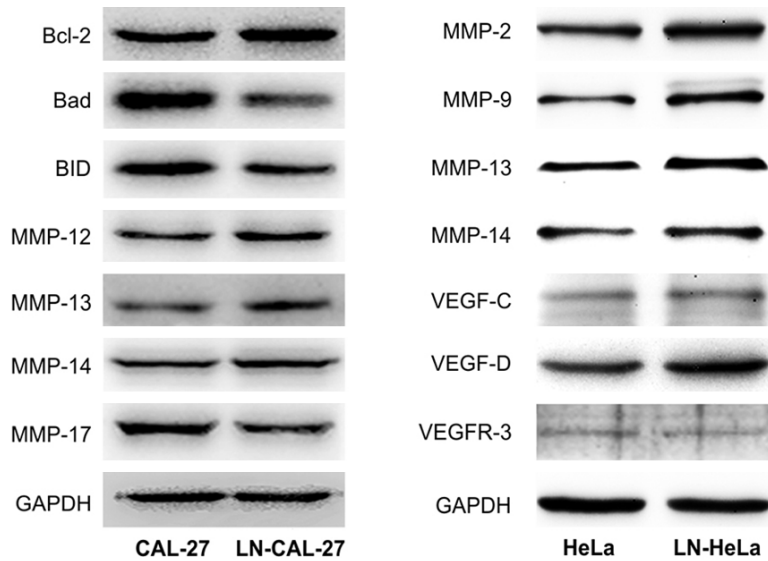


**Figure 4.** Expression of lymphatic metastasis-related proteins in the 2 homologous cell pairs.

speeds of CAL-27 and LN-CAL-27 cells were  $3.76 \pm 0.32 \mu\text{m/h}$  versus  $4.25 \pm 0.11 \mu\text{m/h}$  at 24 h ( $P < 0.05$ ) and  $2.35 \pm 0.10 \mu\text{m/h}$  versus  $2.49 \pm 0.31 \mu\text{m/h}$  at 48 h after wounding; while the HeLa and LN-HeLa cells were  $2.43 \pm 0.29 \mu\text{m/h}$  versus  $3.82 \pm 0.13 \mu\text{m/h}$  at 24 h ( $P < 0.01$ ) and  $2.00 \pm 0.11 \mu\text{m/h}$  versus  $2.69 \pm 0.15 \mu\text{m/h}$  at 48 h ( $P < 0.01$ ) after wounding, respectively. (Figure 3B & 3C).

### Screening SCC lymphatic metastasis-associated genes via the homologous cell pairs by real-time PCR and western blot

To investigate the mechanism underlying SCC lymphatic metastasis, we screened 106 lymphatic metastasis-related genes, including the *MMP*, *VEGF*, *S100*, and chemokine gene families and others by real-time PCR. Fifteen genes in LN-CAL27 cells and 14 genes in LN-HeLa cells were expressed at higher levels than in the parental cell lines. Fifteen genes in both cell pairs showed decreased expression compared to the parental cell lines. Seventeen genes showed consistent expression between the 2 cell pairs (Table 2).

Western blot results correlated with real-time PCR results for *MMP-13* and *MMP-14* expression in CAL-27 and LN-CAL-27 cells and for *MMP-2*, *MMP-9*, *MMP-13*, *MMP-14*, *VEGF-C*, and *VEGFR-3* expression in HeLa and LN-HeLa cells (Figure 4).

### Discussion

Lymph node metastasis is an important stage during the progression of some types of human malignancies, especially for SCC, and influences prognosis and therapeutic design. However, the mechanism underlying lymphatic metastasis remains largely unknown [12]. Given that regional lymph node metastasis is an initial step for SCC metastasis, if the early metastatic step could be controlled, cancer lymphatic metastasis might be avoidable in the future. Therefore, it is necessary to investigate the mechanism underlying cancer lymphatic metastasis. To our

knowledge, one of the main obstacles in lymphatic metastasis research is the lack of reliable in vivo and in vitro lymphatic metastasis models. In this study, we confirmed that the oral lymphatic system is a reliable model for studying SCC lymphatic metastasis and that homologous cell pairs could be established for this system.

Transfected exogenous genes may affect the fate of modified tumor cells [13, 14], leading to poor representation of the natural lymphatic metastasis process of tumor cells. Therefore, we used 3 natural SCC cell lines, CAL-27, Tca-83, and HeLa, to generate orthotopic and xenograft animal models for investigating the mechanism underlying SCC.

The lymphatic metastasis process is a complicated event. To our knowledge, the process could be observed and recorded in very few studies. In this study, we pathologically analyzed lymphatic metastasis. Our results indicate that SCC cells may invade the lymph node by breaking down the lymphatic vessels. Further studies will be required to investigate the mechanism underlying this process.

We established a lymphatic metastasis animal model via the oral lymphatic system and also isolated 2 lymph node metastatic cell lines, LN-CAL-27 and LN-HeLa, after selecting single colonies and culturing them over 60 passages.

## In vivo and in vitro lymphatic metastasis models

We compared the parental cell lines with their corresponding daughter cell lines by STR profiling analysis, cell proliferation, migration ability assays, animal experimentation, real-time PCR, and western blot. The results suggest that the cell pairs are homologous cells with different biological characteristics and lymphatic metastasis ability compared to the parent cell lines. The differential genes and gene products between the 2 homologous cell pairs include the *MMP*, *VEGF*, *S100*, and chemokine families and others (*HIF1 $\alpha$* , *IL-24*, periostin, *TNF $\alpha$* ). These molecular markers could be used to distinguish the daughter cell line from the parental cell line. The *MMP* and *VEGF* families are known to promote metastasis in most cancers [15-20]. Overexpression of *MMPs* could lead to degradation of the extracellular matrix and promote angiogenesis [19]. *VEGFs* could accelerate lymphangiogenesis and facilitate lymphatic metastasis [18]. The interaction of the chemokine family is complicated but important for the lymphatic metastasis [21]. The expression of chemokines was significantly different between the 2 homologous cell pairs; thus, they could be used as an in vitro research tool to study the mechanism underlying lymphatic metastasis. In this study, compared to CAL-27 cells, LN-CAL-27 cells exhibited higher expression of *Bcl-2* and lower levels of *Bad* and *BID*. These results suggest that LN-CAL-27 cells are less likely to undergo apoptosis as *Bcl-2* promotes apoptosis of cells while *Bad* and *BID* inhibit the antiapoptosis [22]. *MMP-14* can activate *MMP-2* protein, and this activity is involved in tumor invasion, which suggests that LN-CAL-27 and LN-HeLa may have better lymphatic metastasis ability than their corresponding parental cells. The expression of *MMP-2* and *VEGF-C* was significantly different between HeLa and LN-HeLa cells but not between CAL-27 and LN-CAL-27 cells. In explanation, we believe that this is attributable to the fact that tumor cells are heterogeneous and behave differently depending on in vivo or in vitro conditions.

In conclusion, SCC lymphatic metastasis is an initial and complicated event during tumor spread. We used 3 cell lines to establish a lymphatic metastasis animal model for oral SCC. The lymphatic metastasis process was observed clearly on serial section analysis of the metastatic lymph node. The establishment of lymphatic metastasis homologous cell lines

using the oral lymphatic system provides a good tool for investigating the cellular changes during the process of SCC lymphatic metastasis and the underlying molecular mechanisms. Further studies are required to determine the lymphatic metastasis mechanisms in the oral lymphatic system and in the lymphatic metastasis homologous cell lines.

### Acknowledgements

The authors would like to thank Dr. Yan Gao for technical support in pathology and Professor Zhong Chen for critical reading of the manuscript. This study is supported by Natural Science Foundation of China (Grant No. 81341062).

### Disclosure of conflict of interest

None.

**Address correspondence to:** Dr. Yi-Xiang Wang, Central Laboratory, Peking University School and Hospital of Stomatology, 22 Zhongguancun Avenue South, Haidian District, Beijing 100081, China. Tel: 86 10 82195537; Fax: 86 10 62173402; E-mail: kqwangyx@bjmu.edu.cn; Dr. Chuan-Bin Guo, Department of Oral and Maxillofacial Surgery, Peking University School and Hospital of Stomatology, 22 Zhongguancun Avenue South, Haidian District, Beijing 100081, China. Tel: 86 10 82195957; Fax: 86 10 62173402; E-mail: guodazuo@sina.com (CBG); puyinfei@yeah.net (YFP)

### References

- [1] Shayan R, Inder R, Karnezis T, Caesar C, Paa-vonen K, Ashton MW, Mann GB, Taylor GI, Achen MG, Stacker SA. Tumor location and nature of lymphatic vessels are key determinants of cancer metastasis. *Clin Exp Metastasis* 2013; 30: 345-356.
- [2] Beltramini GA, Massarelli O, Demarchi M, Coppelli C, Cassoni A, Valentini V, Tullio A, Gianni AB, Sesenna E, Baj A. Is neck dissection needed in squamous-cell carcinoma of the maxillary gingiva, alveolus, and hard palate? A multicentre Italian study of 65 cases and literature review. *Oral Oncol* 2012; 48: 97-101.
- [3] Bagan J, Sarrion G, Jimenez Y. Oral cancer: clinical features. *Oral Oncol* 2010; 46: 414-417.
- [4] Amornphimoltham P, Rechache K, Thompson J, Masedunskas A, Leelahavanichkul K, Patel V, Molinolo A, Gutkind JS, Weigert R. Rab25 regulates invasion and metastasis in head and

## In vivo and in vitro lymphatic metastasis models

- neck cancer. *Clin Cancer Res* 2013; 619: 1375-88.
- [5] Zhang X, Liu Y, Gilcrease MZ, Yuan XH, Clayman GL, Adler-Storthz K, Chen Z. A lymph node metastatic mouse model reveals alterations of metastasis-related gene expression in metastatic human oral carcinoma sublines selected from a poorly metastatic parental cell line. *Cancer* 2002; 95: 1663-1672.
- [6] Lian leB, Tseng YT, Su CC, Tsai KY. Progression of precancerous lesions to oral cancer: results based on the Taiwan National Health Insurance Database. *Oral Oncol* 2013; 49: 427-430.
- [7] Jackson DG. New molecular markers for the study of tumour lymphangiogenesis. *Anticancer Res* 2001; 21: 4279-4283.
- [8] Mandriota SJ, Jussila L, Jeltsch M, Compagni A, Baetens D, Prevo R, Banerji S, Huarte J, Montesano R, Jackson DG, Orci L, Alitalo K, Christofori G, Pepper MS. Vascular endothelial growth factor-C-mediated lymphangiogenesis promotes tumour metastasis. *EMBO J* 2001; 20: 672-682.
- [9] Qiu C, Wu H, He H, Qiu W. A cervical lymph node metastatic model of human tongue carcinoma: Serial and orthotopic transplantation of histologically intact patient specimens in nude mice. *J Oral Maxillofac Surg* 2003; 61: 696-700.
- [10] Myers JN, Holsinger FC, Jasser SA, Bekele BN, Fidler IJ. An orthotopic nude mouse model of oral tongue squamous cell carcinoma. *Clin Cancer Res* 2002; 8: 293-298.
- [11] Sano D, Myers JN. Metastasis of squamous cell carcinoma of the oral tongue. *Cancer Metastasis Rev* 2007; 26: 645-662.
- [12] Tammela T, Alitalo K. Lymphangiogenesis: Molecular mechanisms and future promise. *Cell* 2010; 140: 460-476.
- [13] van Gaal EV, van Eijk R, Oosting RS, Kok RJ, Hennink WE, Crommelin DJ, Mastrobattista E. How to screen non-viral gene delivery systems in vitro? *J Control Release* 2011; 154: 218-232.
- [14] Lv H, Zhang S, Wang B, Cui S, Yan J. Toxicity of cationic lipids and cationic polymers in gene delivery. *J Control Release* 2006; 114: 100-109.
- [15] Lund AW, Duraes FV, Hirosue S, Raghavan VR, Nembrini C, Thomas SN, Issa A, Hugues S, Swartz MA. VEGF-C promotes immune tolerance in B16 melanomas and cross-presentation of tumor antigen by lymph node lymphatics. *Cell Rep* 2012; 1: 191-199.
- [16] Karnezis T, Shayan R, Caesar C, Roufail S, Harris NC, Ardipradja K, Zhang YF, Williams SP, Farnsworth RH, Chai MG, Rupasinghe TW, Tull DL, Baldwin ME, Sloan EK, Fox SB, Achen MG, Stacker SA. VEGF-D promotes tumor metastasis by regulating prostaglandins produced by the collecting lymphatic endothelium. *Cancer Cell* 2012; 21: 181-195.
- [17] Sugiura T, Inoue Y, Matsuki R, Ishii K, Takahashi M, Abe M, Shirasuna K. VEGF-C and VEGF-D expression is correlated with lymphatic vessel density and lymph node metastasis in oral squamous cell carcinoma: Implications for use as a prognostic marker. *Int J Oncol* 2009; 34: 673-680.
- [18] Li B, Li F, Chi L, Zhang L, Zhu S. The expression of SPARC in human intracranial aneurysms and its relationship with MMP-2/-9. *PLoS One* 2013; 8: e58490.
- [19] Kaimal R, Aljumaily R, Tressel SL, Pradhan RV, Covic L, Kuliopulos A, Zarwan C, Kim YB, Sharifi S, Agarwal A. Selective blockade of matrix metalloprotease-14 with a monoclonal antibody abrogates invasion, angiogenesis, and tumor growth in ovarian cancer. *Cancer Res* 2013; 73: 2457-2467.
- [20] Asrani K, Keri RA, Galisteo R, Brown SA, Morgan SJ, Ghosh A, Tran NL, Winkles JA. The HER2- and heregulin  $\beta$ 1 (HRG)-inducible TNFR superfamily member Fn14 promotes HRG-driven breast cancer cell migration, invasion, and MMP9 expression. *Mol Cancer Res* 2013; 11: 393-404.
- [21] Franciszkievicz K, Boissonnas A, Boutet M, Combadiere C, Mami-Chouaib F. Role of chemokines and chemokine receptors in shaping the effector phase of the antitumor immune response. *Cancer Res* 2012; 72: 6325-6332.
- [22] Shamas-Din A, Kale J, Leber B, Andrews DW. Mechanisms of action of Bcl-2 family proteins. *Cold Spring Harb Perspect Biol* 2013; 5: a008714.